

Background

Doxorubicin is member of the anthracycline drug class commonly used to treat a range of cancers. Doxorubicin accumulates in skeletal muscle (1), causing myotoxicity, which can persist long beyond the cessation of treatment (2). Patients treated with doxorubicin experience muscle atrophy (3), weakness and fatigue (4). Impaired contractile function has been reported prior to muscle atrophy (5) and when normalized to muscle cross-sectional area (CSA) (6), thus muscle atrophy alone does not account for the decline in muscle quality.

The concomitant emergence of dysregulated mitochondria following doxorubicin exposure (2, 7, 8) may explain the reduction in skeletal muscle performance, which is dependent upon mitochondrial regulation of cellular energy status and Ca^{2+} handling (9). Loss of mitochondrial quality may therefore be central to understanding doxorubicin-induced myotoxicity. However, the relationship between doxorubicin and loss of skeletal muscle mitochondrial quality remains to be fully understood. This is in part due to a lack of diagnostic analyses assessing doxorubicin-induced skeletal muscle mitochondrial pathology.

The present study was designed to determine the functional impact of acute systemic doxorubicin exposure on skeletal muscle. Measures were conducted 72 hours post-treatment to study the initial phase of dysfunction, prior to extensive muscle wasting, and oxidative damage to proteins and DNA. Fiber-type specific effects were assessed using EDL and soleus muscles due to their divergent fiber-type. In addition, we employed a novel protocol for the assessment of isolated sarcoplasmic reticulum Ca^{2+} uptake across a physiologically relevant spectra of free energies of ATP hydrolysis (ΔG_{ATP}). The study also applied a multiplexed diagnostic assay platform to assess doxorubicin-induced mitochondrial dysfunction under physiological energetic states, which has not previously been explored.

Methods

- Adult C57Bl6/NJ male mice received either a clinically relevant dose of doxorubicin (20mg/kg BM) or equal volume of PBS, delivered via intraperitoneal injection, and were euthanized 72 h later.
- Skeletal muscle function was assessed in two different fiber-type divergent muscles (EDL and soleus) using *in vitro* measures of force, fatigue and contractile kinetics.
- Calcium uptake kinetics were determined fluorometrically using the calcium indicator, Indo-1, with sarcoplasmic reticulum (SR) isolated from hindlimb muscles.
- High-resolution respirometry measures were conducted in isolated mitochondria under multiple substrate conditions using a modified creatine kinase (CK) energetic clamp technique with sequential additions of phosphocreatine (PCr) to assess respiratory control (10).
- Simultaneous measures of mitochondrial membrane potential and NAD(P)H/NAD(P)⁺ redox state were conducted under identical substrate and CK-clamp conditions.
- Maximal enzyme activities were determined colorimetrically, and protein content was assessed in intact isolated mitochondria via native gel.

Discussion and Conclusion

Anthropometric measures and reductions in EDL and soleus specific force agree with previous studies showing EDL contractile decline in the absence of muscle atrophy markers (5, 6). The underlying cause of increased soleus half-relaxation time is likely due to the noted reductions in SR-dependent Ca^{2+} uptake following doxorubicin exposure. Greater calsequestrin content (11) and SERCA activity (12) in the EDL compared to the soleus may have provided protection against a doxorubicin insult in the EDL. Reductions in Ca^{2+} uptake were found across the spectra of ΔG_{ATP} tested, indicating that mechanisms of doxorubicin impairment are not related to abnormal SERCA sensitivity to cellular ΔG_{ATP} .

The substrate-independent nature of the respiratory decline indicates that the limitation is likely not caused by dehydrogenase impairments, nor is it limited to CI or CII. Respiratory sensitivity measures the responsiveness of mitochondria to changes in ΔG_{ATP} . With the exception of R/S, reduced sensitivity was in line with the overall depression in absolute respiration. As such, the respiratory defect is likely not caused by intrinsic limitations to any one ETS component, but the result of fewer functional respiratory complexes and/or a multiplexed lesion across the ETS.

Reduced membrane potential implies that doxorubicin impairs proton pumping or accelerates proton leak. The leftward shift in $\Delta\psi_m$ of the Doxo group, when plotted against JO_2 , is inconsistent with proton leak (i.e., 'uncoupling') and thus supports that the respiratory defect resides in the ETS. Similar NAD(P)H/NAD(P)⁺ levels were observed for both groups under P/M, G/M and Pc/M energized conditions. Plotting JO_2 against pooled NAD(P)H/NAD(P)⁺ revealed no shift in the Doxo group, indicating that the activity of the matrix dehydrogenases were not rate limiting, which was confirmed independently. Quantification of mitochondrial supercomplexes and ATP synthase content/ activity imply that neither ETS complex-interactions or depletion of ETS components are the causes of doxorubicin-induced mitochondrial pathology, and doxorubicin associated defects in respiration are upstream of CV.

Collectively, doxorubicin induces muscle contractile decline that precedes muscle atrophy and is not associated with impaired Ca^{2+} uptake. Muscle contractile dysfunction is associated with lesions likely spanning complexes I-IV of the ETC that may provide potential targets for the alleviation of doxorubicin myotoxicity.

This work was supported by the National Institutes of Health [R01AR06660] (EES).

Results

Figure 1

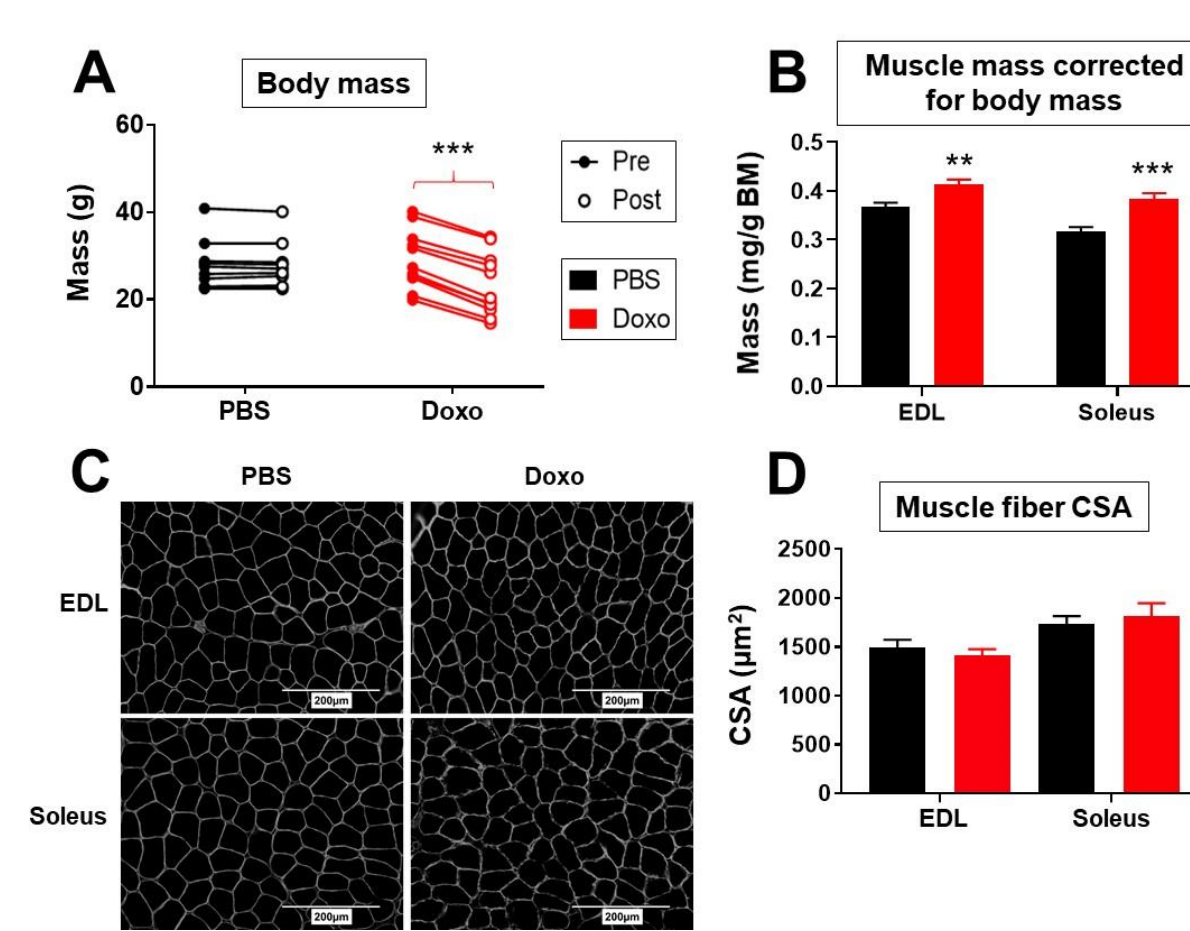


Figure 1. Doxorubicin causes loss of body mass, but does not significantly reduce muscle mass and fiber CSA of EDL and soleus muscles. Changes in body mass following treatment with PBS (n = 10) or Doxo (n = 11) (A). Muscle masses of the EDL and soleus corrected for body mass (PBS, n = 8; Doxo, n = 9) (B). Representative images of EDL and soleus muscle cross-sections (C). EDL and soleus muscle fiber CSA (PBS, n = 4; Doxo, n = 4) (D). **, p < 0.01; ***, p < 0.001. Data are mean ± SEM.

Figure 2

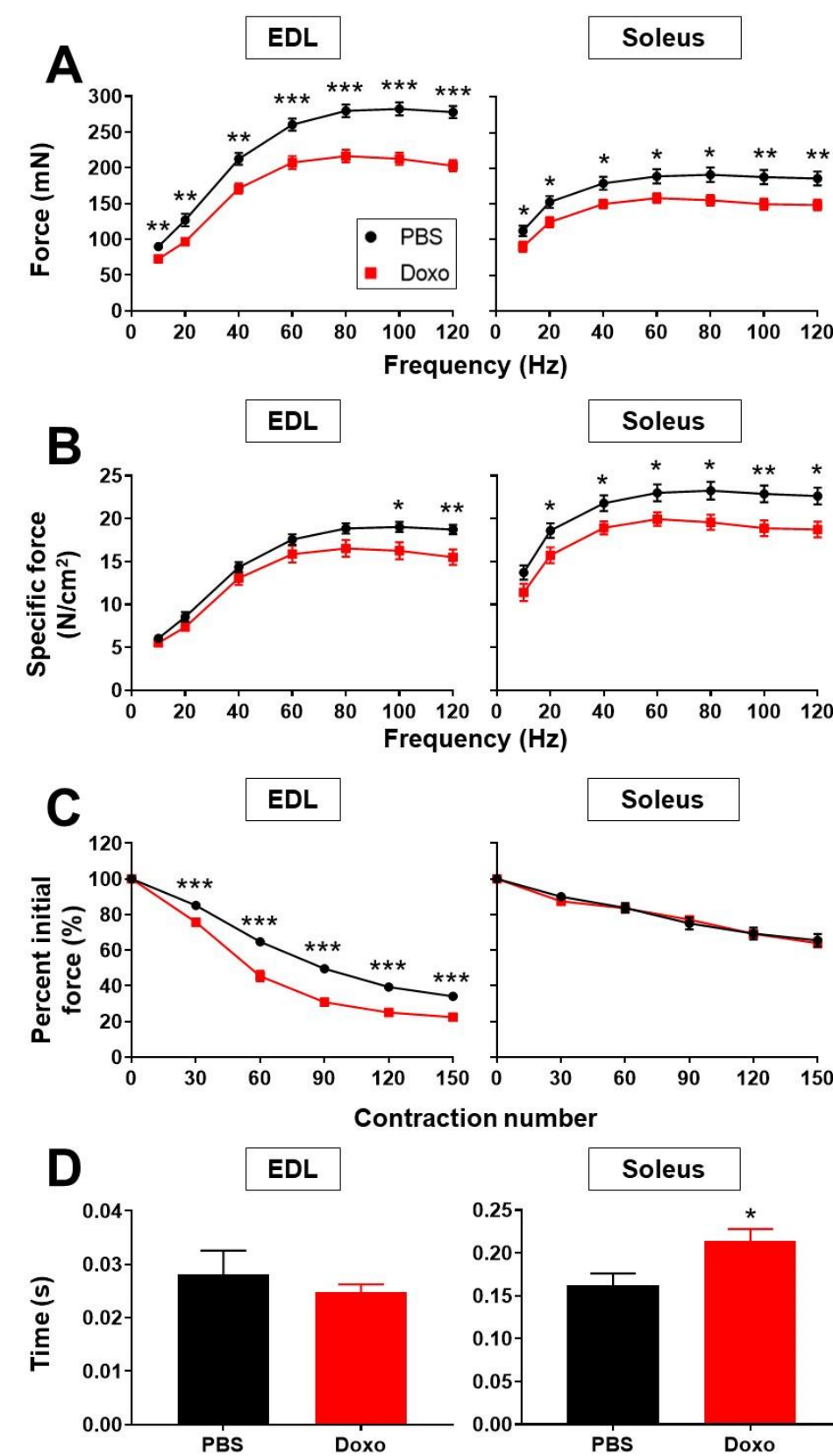


Figure 2. Doxorubicin causes skeletal muscle contractile dysfunction. Force-frequency curve of absolute force (mN) production by EDL and soleus muscles (A). Force-frequency curve of specific force (N/cm²) production by EDL and soleus muscles (B). Muscle fatigue (% change) in the EDL and soleus (C). Half-relaxation time (seconds) of EDL and soleus muscles undergoing a 10 Hz stimulation (D). All measures PBS: n = 8 and Doxo: n = 9. *, p < 0.05; **, p < 0.01; ***, p < 0.001. Data are mean ± SEM.

Figure 3

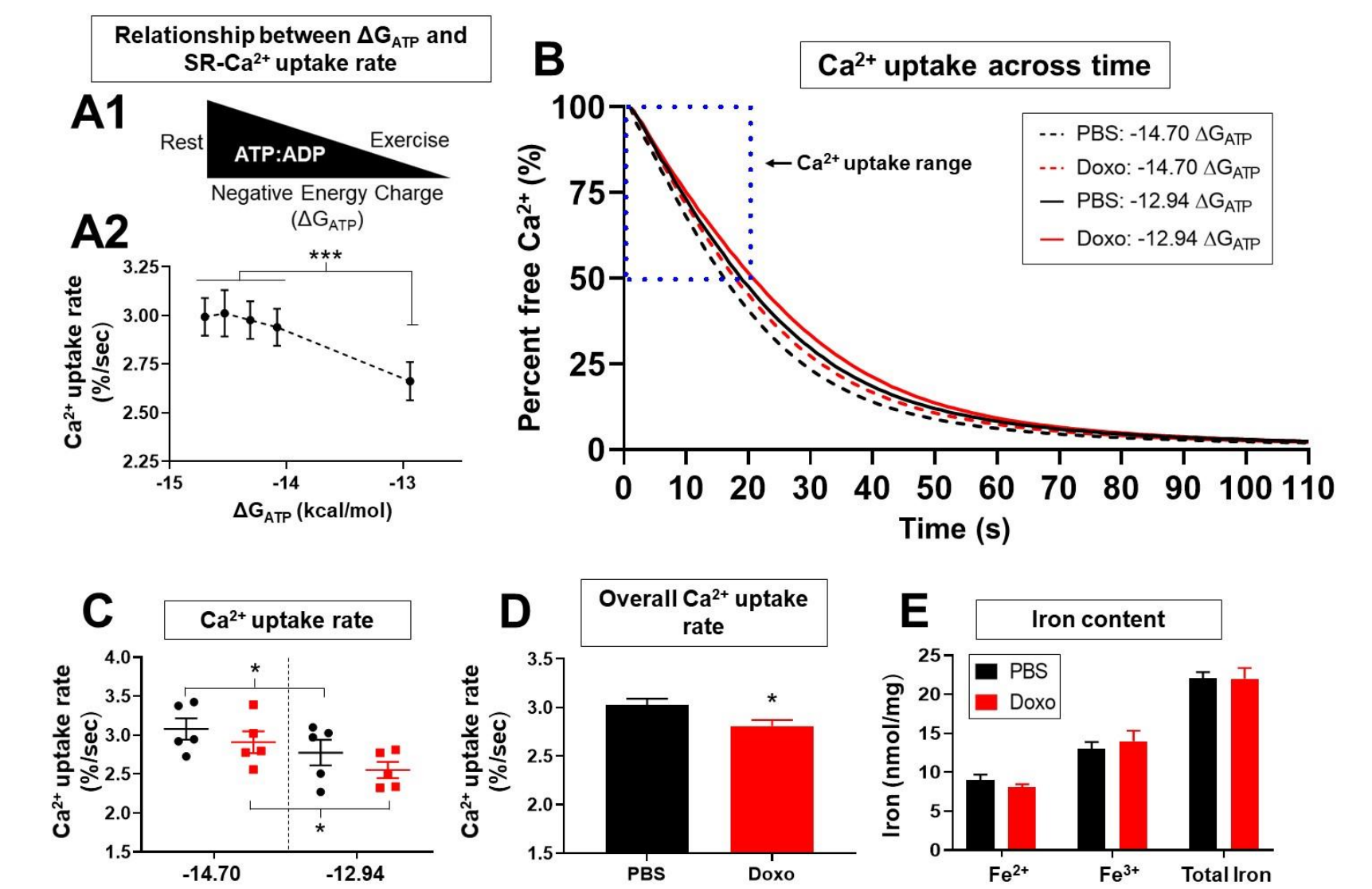


Figure 3. Doxorubicin reduces sarcoplasmic reticulum calcium uptake. Graphic illustrating the relationship between shifts in the ATP/ADP ratio and ΔG_{ATP} (A1). PBS and Doxo Ca^{2+} uptake rates data combined and plotted against ΔG_{ATP} , demonstrating SR- Ca^{2+} uptake rate sensitivity to changes in ΔG_{ATP} (A2). Tracing of percent Ca^{2+} uptake across time by isolated SR under different free energies of ATP hydrolysis (ΔG_{ATP}) (B). Ca^{2+} uptake rate in isolated SR at high (-14.70) and low (-12.94) negative ΔG_{ATP} (C). Overall Ca^{2+} uptake rate averaged across all five ΔG_{ATP} tested (D). Ferrous (Fe^{2+}), ferric (Fe^{3+}) and total iron ($Fe^{2+} + Fe^{3+}$) content of gastrocnemius muscles from PBS and Doxo treated mice (E). All measures PBS: n = 5 and Doxo: n = 5. *, p < 0.05; ***, p < 0.001. Data are mean ± SEM.

Figure 4

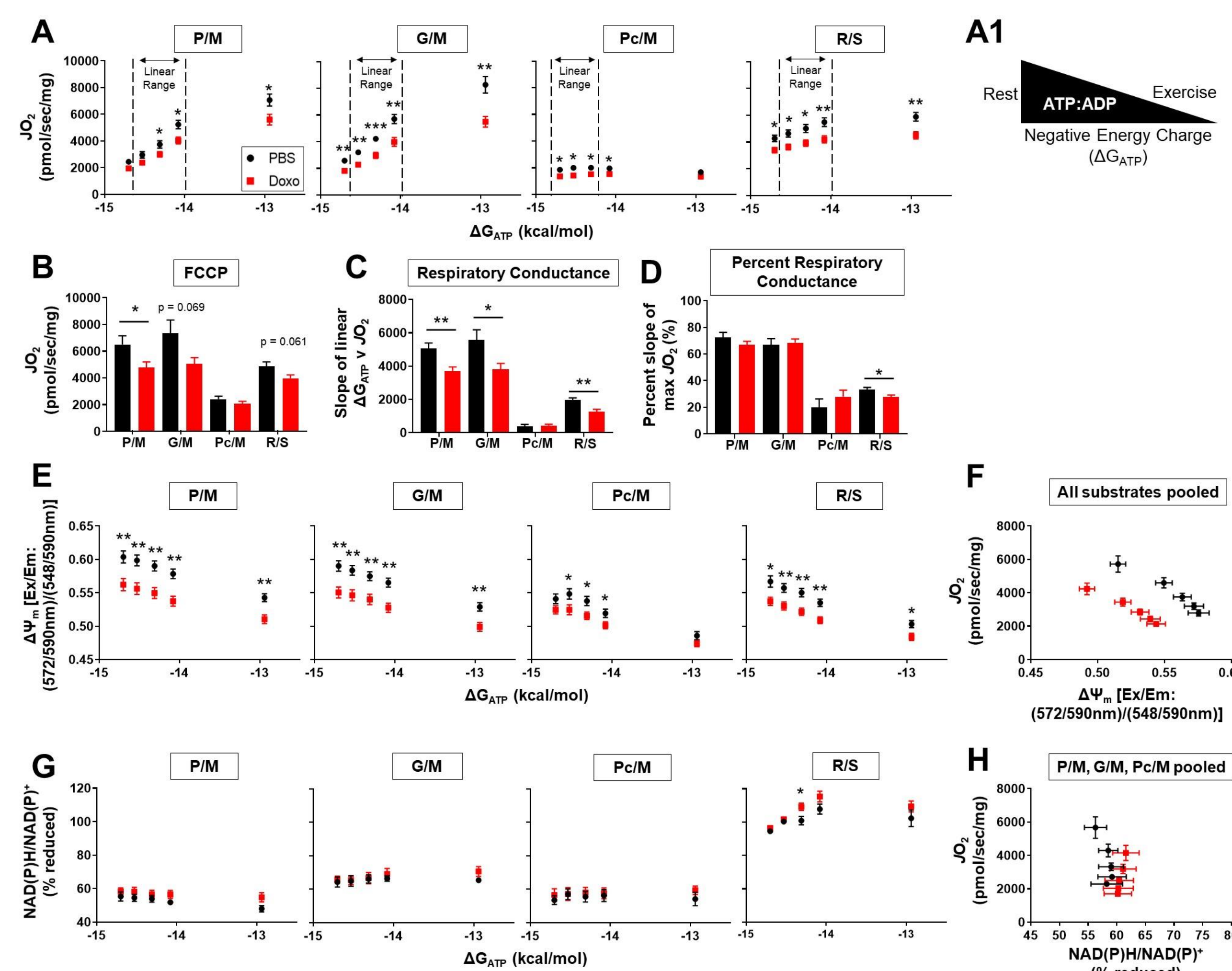


Figure 4. Multiplexed assay platform showing respiratory, membrane potential and NAD(P)H/ NAD(P)⁺ fluxes in response to changing mitochondrial free energies following doxorubicin treatment. Relationship between mitochondrial oxygen consumption (JO_2) (A), membrane potential ($\Delta\psi_m$) (E), and redox status (NAD(P)H/ NAD(P)⁺) (G) versus ATP free energy (ΔG_{ATP}) in isolated mitochondria energized with pyruvate/ malate (P/M), glutamate/ malate (G/M), palmitoyl-carnitine/ malate (Pc/M) and rotenone/ succinate (R/S). Graphic illustrating the relationship between shifts in the ATP/ADP ratio and ΔG_{ATP} (A1). JO_2 following addition of the uncoupling agent, FCCP (B). Respiratory conductance calculated from the slopes of the linear range (dashed lines in A) of JO_2 v ΔG_{ATP} (C). Respiratory conductance normalized to max JO_2 (D). Data from all substrates was pooled to provide an overview of the relationship between JO_2 and $\Delta\psi_m$ (F). Data from P/M, G/M and Pc/M was pooled to provide an overview of the relationship between JO_2 and NAD(P)H/ NAD(P)⁺ (H). All measures PBS: n = 8 and Doxo: n = 8. *, p < 0.05; **, p < 0.01. Data are mean ± SEM.

Figure 6

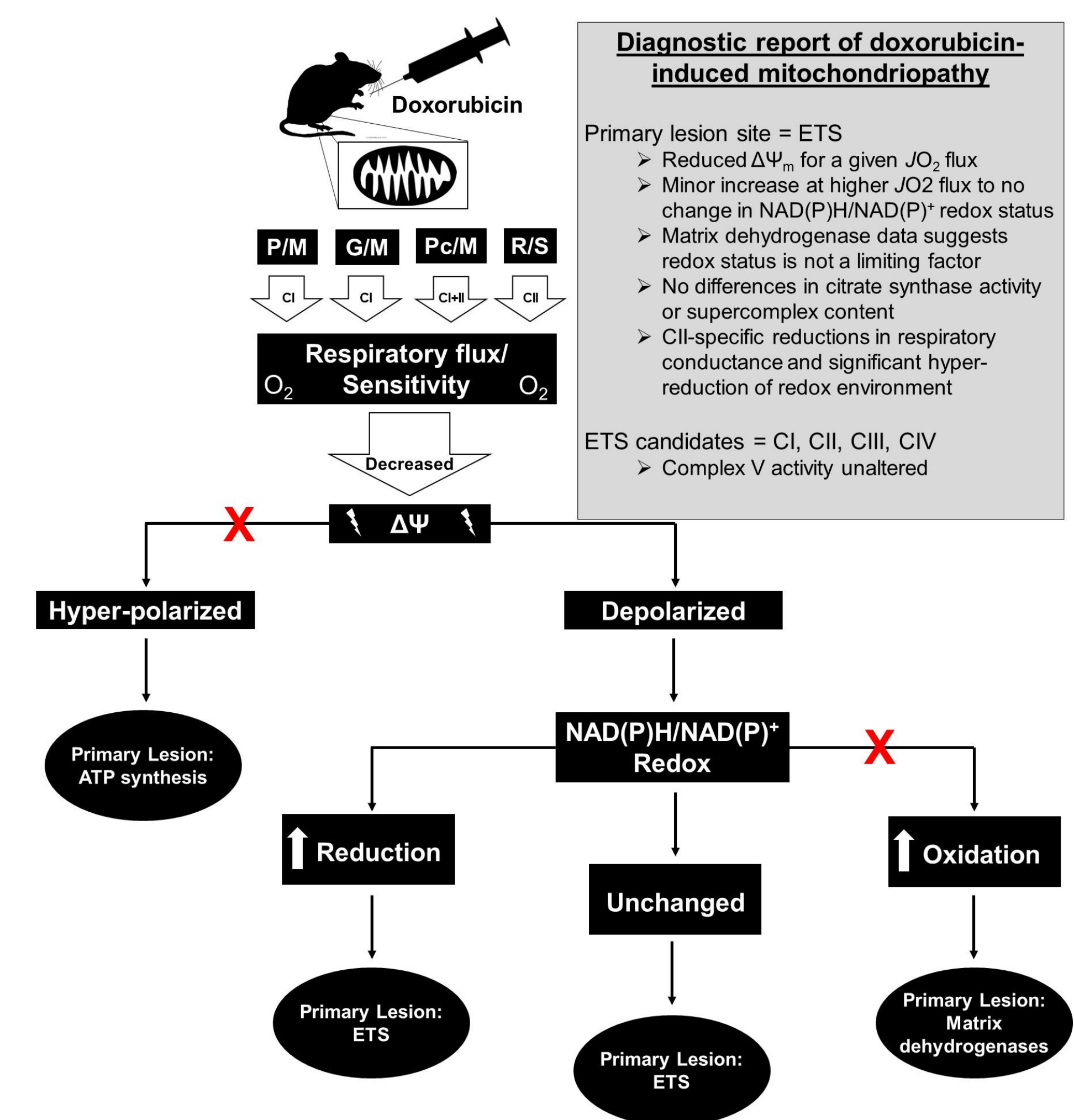


Figure 6. Summary diagnostic work-flow of mitochondria from doxorubicin-treated mice. The summary displays the analytical process of determining potential lesion targets. Overlaying the findings of the current study onto the work-flow reveals that decreased respiratory flux, in conjunction with depolarized membrane potential and reduced/no change in NAD(P)H/ NAD(P)⁺ redox state are symptomatic of lesions to the ETS. Specific targets and supporting evidence are listed in the Diagnostic Report box.

Figure 5

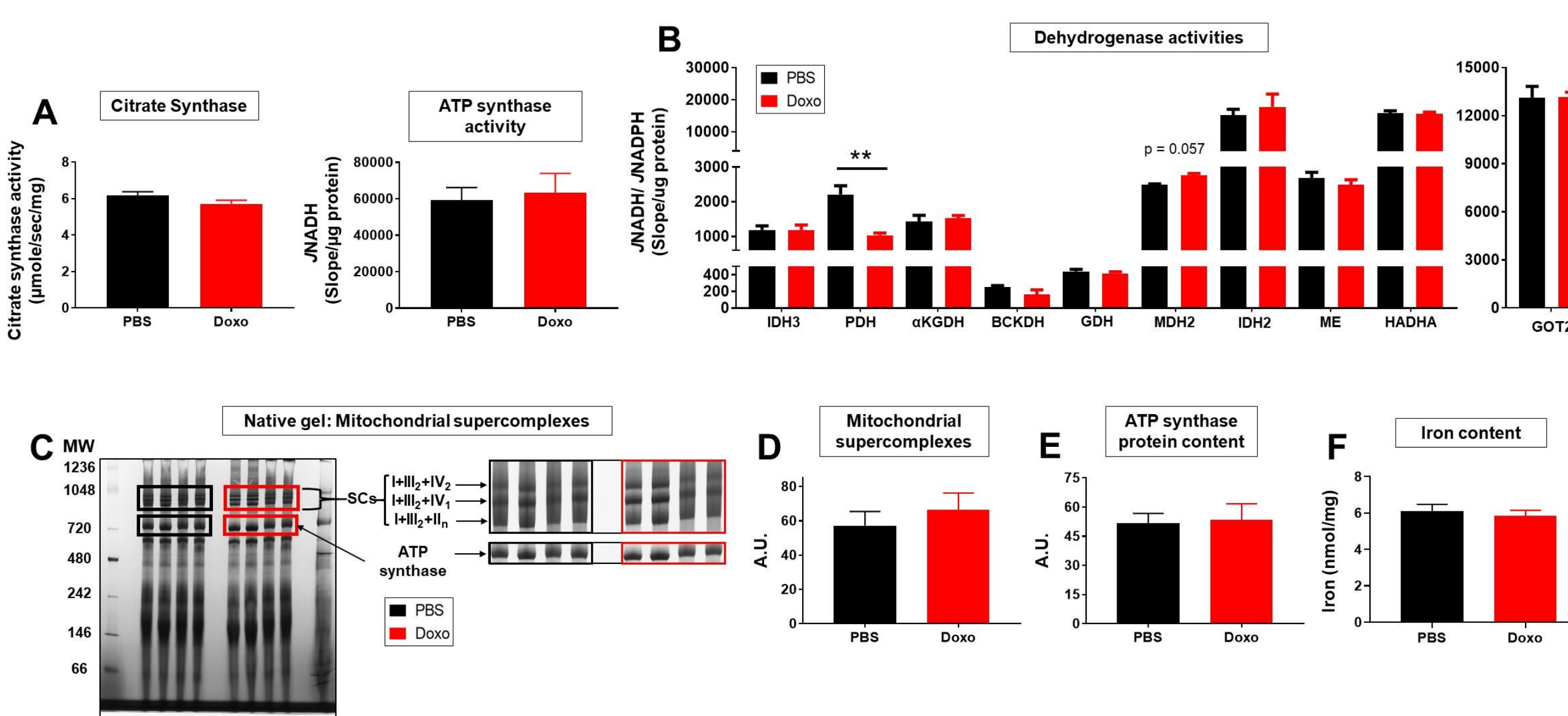


Figure 5. Dehydrogenase flux capacity and mitochondrial content of subunit supercomplexes and ATP synthase. Citrate synthase and ATP synthase (CV) activity rates (A). Enzyme activity rates (J_{NADH}/ J_{NADPH}) of mitochondrial dehydrogenases (isocitrate, IDH3: NAD-linked; pyruvate dehydrogenase complex, PDH; alpha-ketoglutarate dehydrogenase complex, α KGDH; branched-chain keto-acid dehydrogenase complex, BCKDH; glutamate, GDH; malate, MDH2; isocitrate, IDH2: NADP⁺; malic enzyme, ME; hydroxyacyl CoA, HADHA) and aspartate aminotransferase (GOT2) (B). Whole Blue Native PAGE gel and magnified inset showing mitochondrial supercomplexes and ATP synthase protein content (C). Doxorubicin did not alter the protein content of mitochondrial supercomplexes I+III₂+IV₂, I+III₂+IV₁, I+III₂+I₁ (D), or ATP synthase (E). Total iron ($Fe^{2+} + Fe^{3+}$) content of isolated mitochondria from PBS (n = 4) and Doxo (n = 3) treated mice was similar between groups (F). All measures PBS: n = 4 and Doxo: n = 4 unless otherwise stated. **, p < 0.01. Data are mean ± SEM.

References

- Fabris, S., and MacLean, D. A. (2015) Skeletal Muscle an Active Compartment in the Sequestering and Metabolism of Doxorubicin Chemotherapy. *PLoS One*, 10, e0119070
- Goussipoulou, G., Scheede-Bergdahl, C., Spendiff, S., Vuda, M., Meehan, B., Mlynarski, H., Archer-Lahou, E., Sgarbi, N., Puvres-Smith, F. M., Konokhova, Y., Rak, J., Chevalier, S., Taivassalo, T., Hepple, R. T., and Jagoe, R. T. (2015) Anthracycline-containing chemotherapy causes long-term impairment of mitochondrial respiration and increased reactive oxygen species release in skeletal muscle. *Sci. Rep.* 5, 8717
- Bonifati, D. M., Ori, C., Rossi, C., Cairra, S., Fanin, M., and Angelini, C. (2000) Neuromuscular damage after hyperthermic isolated limb perfusion in patients with melanoma or sarcoma treated with chemotherapeutic agents. *Cancer Chemother. Pharmacol.* 46, 517-522
- Jacobsen, P. B., Hann, D. M., Azzarello, L. M., Horton, J., Balducci, L., and Lyman, G. H. (1999) Fatigue in women receiving adjuvant chemotherapy for breast cancer: characteristics, course, and correlates. *J. Pain Symptom Manage.* 18, 233-42
- Bredahl, E. C., Pfannenstiel, K. B., Quinn, C. J., Hayward, R., and Hydock, D. S. (2016) Effects of Exercise on Doxorubicin-Induced Skeletal Muscle Dysfunction. *Med. Sci. Sport. Exerc.* 48, 1468-1473
- Gilliam, L. A. A., Ferreira, L. F., Bruton, J. D., Moylan, J. S., Westerblad, H., St Clair, D. K., and Reid, M. B. (2009) Doxorubicin acts through tumor necrosis factor receptor subtype 1 to cause dysfunction of murine skeletal muscle. *J. Appl. Physiol.* 107, 1935-42
- Gilliam, L. A. A., Larik, D. S., Reese, L. R., Torres, M. J., Ryan, T. E., Lin, C.-T., Cathey, B. L., and Neuffer, P. D. (2016) Targeted overexpression of mitochondrial catalase protects against cancer chemotherapy-induced skeletal muscle dysfunction. *Am. J. Physiol. Endocrinol. Metab.* 311, E293-301
- A Gilliam, L. A., Fisher-Wellman, K. H., Lin, C.-T., Maples, J. M., Cathey, B. L., and Darrell Neuffer, P. (2013) The anticancer agent doxorubicin disrupts mitochondrial energy metabolism and redox balance in skeletal muscle. 10.1016/j.freeradbiomed.2013.08.191
- Rossi, A. E., Boncompagni, S., and Dirksen, R. T. (2009) Sarcoplasmic reticulum-mitochondrial symbiosis: bidirectional signaling in skeletal muscle. *Exerc. Sport Sci. Rev.* 37, 29-35
- Fisher-Wellman, K. H., Davidson, M. T., Narowski, T. M., Lin, C.-T., Koves, T. R., and Muoio, D. M. (2018) Mitochondrial Diagnostics: A Multiplexed Assay Platform for Comprehensive Assessment of Mitochondrial Energy Fluxes. *Cell Rep.* 24, 3593-3606.e10
- Murphy, R. M., Larkins, N. T., Mollica, J. P., Beard, N. A., and Lamb, G. D. (2009) Calsequestrin content and SERCA determine normal and maximal Ca^{2+} storage levels in sarcoplasmic reticulum of fast- and slow-twitch fibres of rat. *J. Physiol.* 587, 443-460
- Lohr, M. J., Lucas-Heron, B., Olivier, B., and Leoty, C. (1998) Calcium binding protein changes of sarcoplasmic reticulum from rat denervated skeletal muscle. *Biochim. Biophys. Acta* 142, 369-78